



Infrared spectra of the main optical properties of poly(methyl methacrylate) thin films

Maria Laura Strugariu¹ · Sorina Gabriela Șerban¹ · Antonia Maria Berdie² · Simion Jitian¹

Received: 3 December 2023 / Revised: 13 February 2024 / Accepted: 18 March 2024 /
Published online: 6 April 2024

© The Author(s), under exclusive licence to Springer-Verlag GmbH Germany, part of Springer Nature 2024

Abstract

This study aimed to determine the infrared (IR) spectra of the main optical properties of poly(methyl methacrylate) (PMMA). This is a simple and original method for obtaining spectra of the main optical properties from the reflection–absorption spectrum. Infrared reflection spectra of the main optical properties of PMMA were obtained from the complex relative permittivity using the Drude–Lorentz model for permittivity. Classical dispersion analysis of the reflection–absorption spectrum of poly(methyl methacrylate) films cast on a metal mirror was performed. The method is based on an iterative least squares fitting process of the experimental reflection–absorption spectrum of the polymer with the corresponding theoretical spectrum obtained from the complex permittivity Drude–Lorentz model. This approach is original for obtaining the relative permittivity and subsequently obtaining the main optical properties of the polymer film: complex electric modulus, energy loss function, optical constants, absorption coefficient, penetration depth, dissipation factor, and complex optical conductivity. In addition to the findings of other articles, some optical properties of PMMA films have been presented, which may be useful for studying PMMA-based composites or copolymers.

Keywords Infrared spectra · Poly(methyl methacrylate) · Optical properties · Classical dispersion analysis · Complex relative permittivity · Complex electric modulus · Energy loss function · Optical constants · Absorption coefficient · Penetration depth · Dissipation factor · Complex optical conductivity

✉ Simion Jitian
jitian_s@yahoo.com

¹ Department of Engineering and Management, Polytechnica University, Timișoara 5 Revoluției Str., 331128 Hunedoara, Romania

² Department of Conservation and Restoration, Faculty of Graphic Arts, Art and Design University, Piața Unirii Nr.31, 400098 Cluj-Napoca, Romania

Introduction

Thermoplastic poly(methyl methacrylate) (PMMA) has good hardness and tensile strength, high stiffness, transparency, strong insulating qualities, and temperature stability that depend on tacticity. The optical qualities are excellent. For a variety of optical applications, determining the optical characteristics is crucial. Microelectronics, nonlinear optics, optical accessories, food packaging, dentistry, and cosmetics are just a handful of the many industries that use this polymer or its copolymers. Reflection and transmission techniques, such as Fourier transform infrared (FTIR) spectroscopy and Kramers–Kronig analysis, are often used to obtain infrared spectra of the optical constants n and k [1–3].

Method

Another method, classical dispersion analysis, was used successfully in this paper to process the infrared reflection–absorption spectra of thin PMMA superficial films. This approach is original and allows us to easily determine the main optical properties of superficial polymer films.

The measured spectrum is a transfection spectrum. The measured size was the transmittance. The resulting transfection spectra are similar to the transmission spectra [4, 5].

Classical dispersion analysis relies on the Drude–Lorentz model of independent oscillators. This model describes complex relative permittivity using the following equation:

$$\tilde{\epsilon}_r(\nu) = \frac{\tilde{\epsilon}(\nu)}{\epsilon_0} = \epsilon_\infty + \sum_j \frac{\nu_{pj}^2}{\nu_{0j}^2 - \nu^2 - i\gamma_j\nu} \quad (1)$$

Each oscillator is represented by a Lorentzian with three adjustable parameters: the oscillator frequency ν_{0j} , the line width γ_j and the plasma frequency ν_{pj} . The parameter ϵ_∞ is the contribution of higher frequency oscillators. The parameter ϵ_0 is the vacuum permittivity ($=8.854 \times 10^{-12}$ F/m), and ϵ_∞ is the contribution of the higher frequency oscillators [6].

The fitting process consists of introducing into the expression of relative permittivity described by the Drude–Lorentz equation the dispersion parameters ϵ_∞ , ν_0 , ν_p and γ corresponding to the independent oscillators of the different groups in the polymer structure and adjusting them until the transmittance T_{model} obtained from the modeled relative permittivity approximates the best experimental transmittance corresponding to the reflection–absorption spectrum of the polymer [4, 5, 7].

The relative permittivity $\tilde{\epsilon}_r$ of Eq. (1) is continuously modified by adjusting the parameters ϵ_∞ , ν_0 , ν , and γ until a minimum value of the quantity χ^2 is obtained:

$$\chi^2 = \sum_j^N \left(\frac{y_j - f(x_j, p_1, \dots, p_M)}{\sigma_j} \right)^2 = \chi^2(p_1, \dots, p_M) \tag{2}$$

The chi-square test calculates the sum of the squares of the differences divided by the standard deviation between the experimental and model transmittance values.

In this equation, y_j is the experimental transmittance at different frequencies ν , and $f(x_j, p_1, \dots, p_M)$ corresponds to the transmittance of the model at the same frequencies. σ_i provides the standard deviation. The Levenberg–Marquardt algorithm, also known as the damped least squares method, was used [6].

The complex relative permittivity was obtained using classical dispersion analysis based on a previously described model (Drude–Lorentz). This quantity is the basis for the subsequent determination of the main optical properties based on the relationships between them, according to the scheme shown in Fig. 1.

Expression of the main optical properties versus the relative permittivity

The novelty of this work lies in the simple way of obtaining infrared (IR) spectra of the main optical properties. They are obtained from infrared spectra of complex relative permittivity $\tilde{\epsilon}_r = \epsilon_1 + i\epsilon_2$, obtained by classical dispersion analysis of the infrared (IR) reflection–absorption spectra of PMMA thin films. The relationships between them were evaluated. All these quantities depend on the temperature and frequency of the radiation. Thus, the spectra of these quantities are obtained.

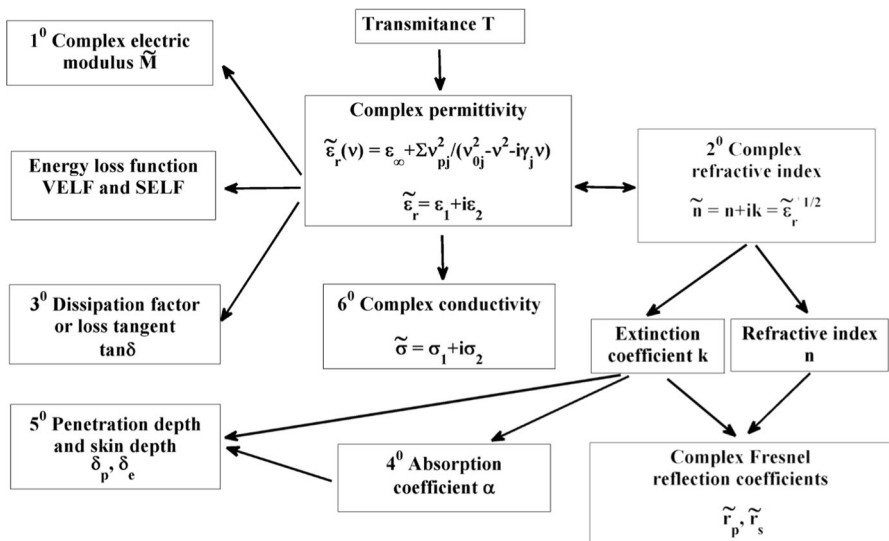


Fig. 1 Overview of the main optical properties of the polymer film obtained from the complex permittivity obtained by classical dispersion analysis of the infrared reflection–absorption spectrum of polymers

The complex electric modulus \tilde{M}

The reciprocal of the complex relative permittivity is the complex electric modulus [8, 9]. This provides a clearer characterization of the dipolar relaxation mechanisms of polymeric films. Equation (3) shows the equation that defines the complex electric modulus \tilde{M}

$$\tilde{M} = \frac{1}{\tilde{\epsilon}_r} = M_1 + iM_2 = \frac{\epsilon_1}{\epsilon_1^2 + \epsilon_2^2} + i \frac{\epsilon_2}{\epsilon_1^2 + \epsilon_2^2} \quad (3)$$

The imaginary part of the complex electric modulus M_2 was calculated in the RefFIT program [10] as a loss function L_f or was defined as a volume (bulk) energy loss function, VELF [11–13]. The energy loss function (ELF) describes the energy lost while passing through the film. The ELF has two main sections: the surface energy loss function (SELF) and the volume energy loss function (VELF). The surface energy loss function (SELF) and the volume energy loss function (VELF) are two components of the energy loss function. The ELF is the sum of the two quantities, both of which are obtained from ϵ_1 and ϵ_2 . The real part ϵ_1 refers to the dispersion, and ϵ_2 refers to the absorption of light waves in the optical medium. The following relations provide the two terms of ELF.

$$\begin{aligned} M_2 = \text{VELF} &= \text{Im}\left(-\frac{1}{\tilde{\epsilon}_r}\right) = \frac{\epsilon_2}{\epsilon_1^2 + \epsilon_2^2} = L_f; \\ \text{SELF} &= \text{Im}\left(-\frac{1}{\tilde{\epsilon}_r} + 1\right) = \frac{\epsilon_2}{(\epsilon_1^2 + 1)^2 + \epsilon_2^2} \end{aligned} \quad (4)$$

The complex refractive index \tilde{n}

The complex refractive index is obtained from the complex relative permittivity value with the following equation:

$$\tilde{n} = n + ik = \sqrt{\tilde{\epsilon}_r} \quad (5)$$

The refractive index n , which is the real part of the complex refractive index, describes the dispersive properties of the material. It can be calculated from the complex permittivity [14, 15].

$$n = \text{Re}(\tilde{\epsilon}_r) = \sqrt{\frac{1}{2}\left(\sqrt{\epsilon_1^2 + \epsilon_2^2} + \epsilon_1\right)} \quad (6)$$

The extinction coefficient k is the imaginary part of the complex refractive index that describes the absorbing properties of the material and can be calculated from the complex permittivity with the following equation:

$$k = \text{Im}(\tilde{\epsilon}_r) = \sqrt{\frac{1}{2} \left(\sqrt{\epsilon_1^2 - \epsilon_2^2} - \epsilon_1 \right)} = \frac{\epsilon_2}{2n} \tag{7}$$

Dissipation factor (or dielectric loss tangent) $\tan \delta$

The dissipation factor (also known as the dielectric loss tangent) can be used to describe how much energy dissipates inside the polymer after interaction with an electromagnetic wave. The loss tangent $\tan \delta$ is used to investigate how well a material can absorb an electromagnetic field [8, 9, 13, 21]. It is defined as the ratio of the imaginary part to the real part of the complex relative permittivity.

$$\tan \delta = \frac{\epsilon_2}{\epsilon_1} \tag{8}$$

The absorption coefficient α

The absorption coefficient is obtained from the extinction coefficient. This allows us to measure how much light is absorbed by a material. [11–13, 16–20].

$$\alpha = \frac{4\pi}{\lambda} k = 2 \frac{\omega}{c} k \tag{9}$$

Penetration depth δ_p and skin depth δ_e

When radiation is reflected on the surface that separates two different media, part of the radiation is reflected, and the other part is absorbed in the medium in which it is refracted. The depth at which the intensity or power of the field within the material decays to 1/e of its surface value is defined as the penetration depth [22]. The skin depth δ_e is the depth at which the intensity of the electric field drops to 1/e of its value at the surface.

$$\delta_p = \frac{1}{\alpha} = \frac{\lambda}{4\pi k} ; \delta_e = \frac{2}{\alpha} = 2\delta_p \tag{10}$$

Skin depth is sometimes called the penetration depth.

Complex optical conductivity $\tilde{\sigma}$

The complex optical conductivity measures the response of a material to light and is related to the complex relative permittivity $\tilde{\epsilon}_r$, [11–13, 19, 23–27]. The complex permittivity describes how much electrons displace when the field is applied, whereas the complex conductivity describes how fast electrons move under the influence of the applied field. The complex optical conductivity $\tilde{\sigma} = \sigma_1 + i\sigma_2$ can provide details about the structural and optoelectronic properties of the material.

The imaginary part of the complex permittivity ε_2 that determines the absorption of the wave inside the medium contributes to the real part of the optical conductivity $\sigma_1 = \varepsilon_0 \omega \varepsilon_2$, and the real part of the complex permittivity ε_1 that expresses the dispersive properties of the medium contributes to the imaginary part of the optical conductivity $\sigma_2 = \varepsilon_0 \omega \varepsilon_1$

$$\tilde{\varepsilon} = \varepsilon_0 \tilde{\varepsilon}_r = \varepsilon_0 (\varepsilon_1 + i\varepsilon_2) = \varepsilon_0 + \frac{i\sigma}{\omega} = \varepsilon_0 \left(1 + \frac{i\sigma}{\varepsilon_0 \omega} \right) \quad (11)$$

$$\sigma_1 = \varepsilon_0 \omega \varepsilon_2; \sigma_2 = \varepsilon_0 \omega \varepsilon_1 \quad (12)$$

In this equation, ω is the angular frequency (rad/s). Aly [28] presented a critical comment related to the correct expression of optical conductivity in the International System of Units.

Experimental

The highly polished surface of a steel sample was used as a substrate. Then, a poly(methyl methacrylate) (PMMA) solution was added to the metal substrate at a concentration of approximately 3.3 g/L [4]. A good solvent used for PMMA was benzene [29]. Spin coating techniques [30–33] or dip coating [34, 35] are commonly used to obtain thin films on surfaces. However, they can induce a certain orientation of the polymer chain during polymer film casting. Dropcasting was the deposition technique used to create thin films. To create films with thicknesses on the order of micrometers, polymer solutions with a concentration of approximately 3.3 g/L were dropped onto the horizontal surface of the metal mirrors. A Griffin beaker was applied to the sample, onto which the polymer solution was poured. The function of the beaker was to slow the evaporation rate of the solvent to produce uniformly thick surface coatings. Below the spill mouth of the Griffin beaker, the solvent in the polymer solution was slowly evaporated into a saturated atmosphere of solvent vapor. Thus, superficial films of controlled and uniform thickness are obtained on the entire surface of the metallic mirror [7]. Atactic poly(methyl methacrylate) granules without further purification (Montedison, Italy Mw ~ 97 kg/mol by GPC, Mn ~ 46 kg/mol, Tg = 105 °C, Tm = 150 °C) were used to prepare the polymer solutions.

The surface film deposited on the metal mirror was lightly heated to a temperature of 80 °C for 30 min to completely remove the residual solvent. The presence of residual solvent can cause changes in the appearance of the polymer spectrum [36]. Due to the heating of the samples after deposition of the polymer film at 80 °C for 30 min, we considered that the solvent was removed from the surface film. The benzene absorption band at 669.5 cm⁻¹ [36], which may indicate the presence of benzene, is not observed in the spectrum of the analyzed PMMA film. As shown in Serban et al. [36], for thin films with micron thicknesses, the solvent is removed under the experimental conditions used.

The IR reflection–absorption spectrum of the PMMA thin film was recorded at a 20-degree incidence angle within the spectral range of 500–4000 cm⁻¹ using the

specular reflectance device of the Carl Zeiss Jena UR-20 spectrophotometer. The experimental error bar for the measured infrared reflection–absorption (IRRA) spectrum was 0.01.

The RefFIT calculation program was used to obtain the dielectric function and the theoretical spectrum of the PMMA film based on the Drude–Lorentz model with classical dispersion analysis [10]. The experimentally obtained spectrum and the theoretical spectrum were fitted by iterative adjustment of the model parameters. A superficial film thickness of 10.6 μm was obtained. Since incident radiation, after reflection on the metal mirror, crosses the polymer film twice, 5.3 μm was considered its thickness. The thickness obtained corresponds to the concentration of the polymer in the benzene solution. A total of 27 damped harmonic oscillators were used to fit the polymer model spectrum to the experimental spectrum of the polymer, digitized at 3501 experimental points [4].

Results and discussion

The RefFIT computation program was applied to process the reflection–absorption spectrum (RAS) of the superficial PMMA layer that was placed on the metallic steel mirror. The program uses classical dispersion analysis based on the Drude–Lorentz model according to relation (1) [6]. In addition to [4], Fig. 2 shows the mid-infrared region (500–4000 cm^{-1}) of the two PMMA surface film spectra: the experimental reflection–absorption spectrum and the model transmission spectrum based on the Drude–Lorentz Eq. (1). Very good matching of the two spectra over the entire analyzed spectral domain is observed. In paper [4], only a detail of this spectral range is presented to highlight the good approximation of the theoretical spectrum to the experimental one.

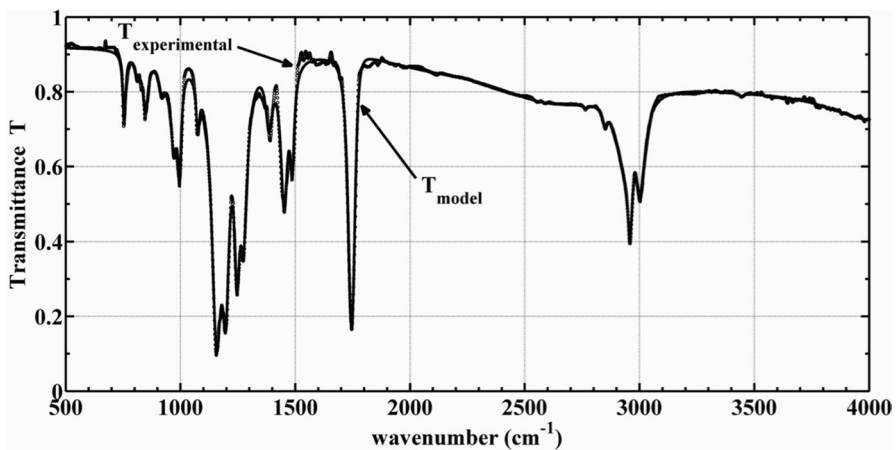


Fig. 2 Comparison of the experimental infrared reflection–absorption spectrum $T_{\text{experimental}}$ with the transmission model spectrum T_{model} obtained by classical dispersion analysis with the RefFIT program for poly(methyl methacrylate) films

Equation (2) indicates that the lowest value of quantity χ^2 for the 3501 experimental points of the spectrum was 1954.56, based on the fitting of these spectra.

The complex relative permittivity $\tilde{\epsilon}_r$ and thickness of the superficial film of PMMA deposited from a benzene solution on the surface of a steel mirror were obtained by fitting the Drude–Lorentz model of the transmission spectrum with that of the experimental reflection–absorption spectrum. A good fit of the model built with the experimental spectrum was observed.

Figure 3 shows the infrared spectra of the real and imaginary parts of a PMMA film cast from solutions on a metallic steel mirror. Using fitting, the thickness of the surface film was determined to be 5.3 μm .

Figure 4 shows the real and imaginary parts of the complex electric modulus $\tilde{M} = \frac{1}{\tilde{\epsilon}_r} = M_1 + iM_2$, expressed in relation (3).

The IR spectra of the real and imaginary parts of the complex relative permittivity and complex electric modulus are similar.

The loss function L_f defined by Kuzmenko [10] and the imaginary part M_2 of the complex electric modulus are the same as the VELF reported by El-Nahass et al. [11].

Figure 5 shows the two components of the energy loss function for the PMMA film cast on the metallic mirror: the volume energy loss function (VELF) and the surface energy loss function (SELF), which are determined by Eq. (4).

The SELF describes the inelastic reflection of electrons on the flat surface of a solid without accounting for spatial dispersion. The SELF represents the energy loss by free charge carriers when traversing the surface of the material [13].

The ratio of the two components of the energy loss function VELF/SELF is shown in Fig. 6. In the spectral regions where the superficial film shows high absorption, high values of this ratio are obtained.

The refractive index n and the extinction coefficient k are obtained from the complex relative permittivity based on Eqs. (5–7). Figure 6 shows the infrared spectra

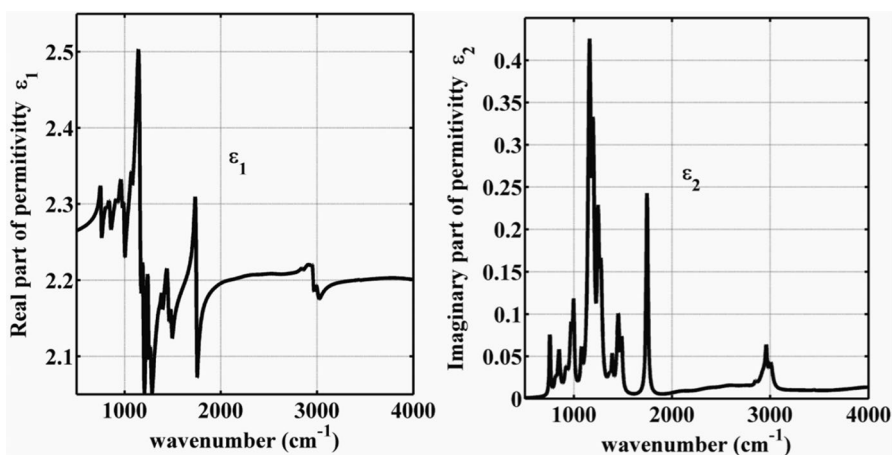


Fig. 3 Infrared spectra of the real part ϵ_1 and the imaginary part ϵ_2 of the complex relative permittivity for the superficial poly(methyl methacrylate) film cast on a metal mirror

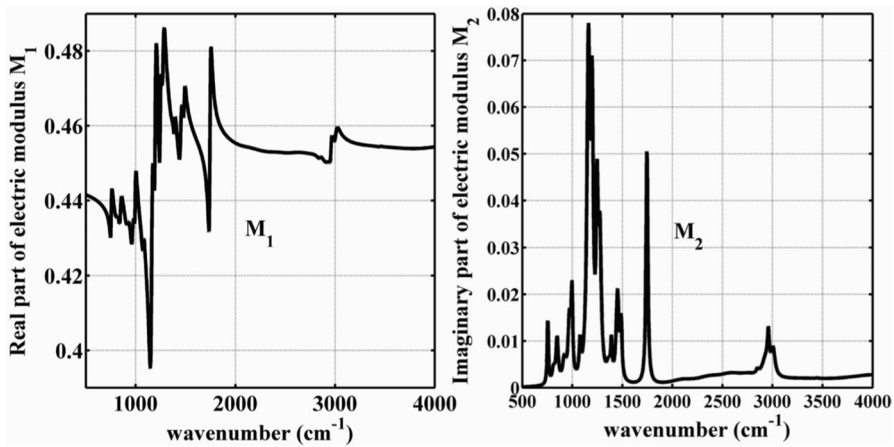


Fig. 4 Infrared spectra of real part M_1 and imaginary part M_2 of the complex electric modulus of the superficial poly(methyl methacrylate) film cast on a metallic mirror

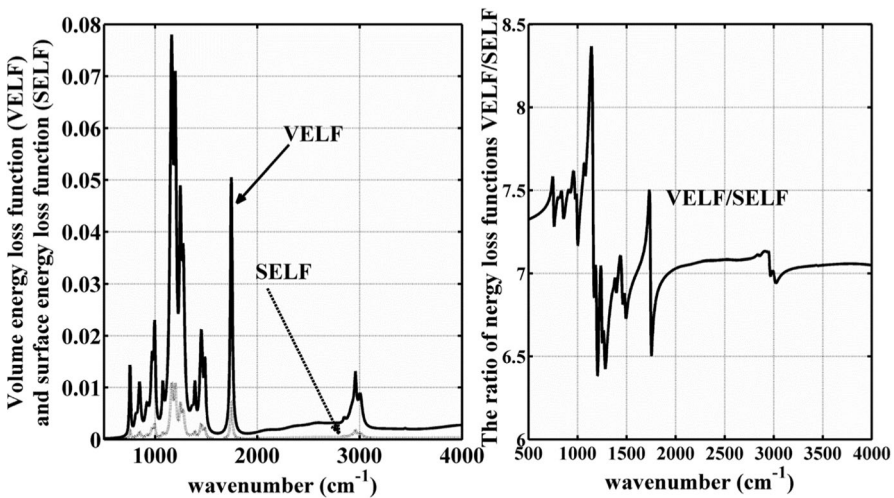


Fig. 5 Infrared spectra of the energy loss functions and the ratio of the two components, the volume energy loss function (VELF) and the surface energy loss function (SELF) for the poly(methyl methacrylate) film cast on the metallic mirror

of the refractive index n and the extinction coefficient k of the PMMA film cast on a metal mirror.

A more detailed presentation of these optical constants can be found in [4]. The frequencies of the intense peaks in the IR extinction coefficient spectrum are also presented. Figure 7 shows the IR spectrum of the dissipation factor $\tan \delta$ of the PMMA film cast on the metal mirror.

This spectrum is similar to that of the imaginary part ϵ_2 of the complex permittivity. Equation (8) expresses the absorption coefficient α as a function of

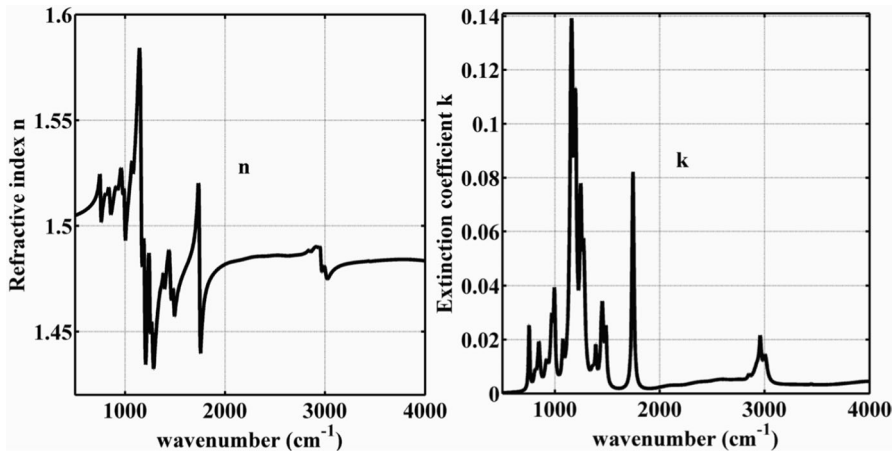


Fig. 6 Infrared refractive index n and extinction coefficient k spectra of the poly(methyl methacrylate) film cast on a metal mirror [4]

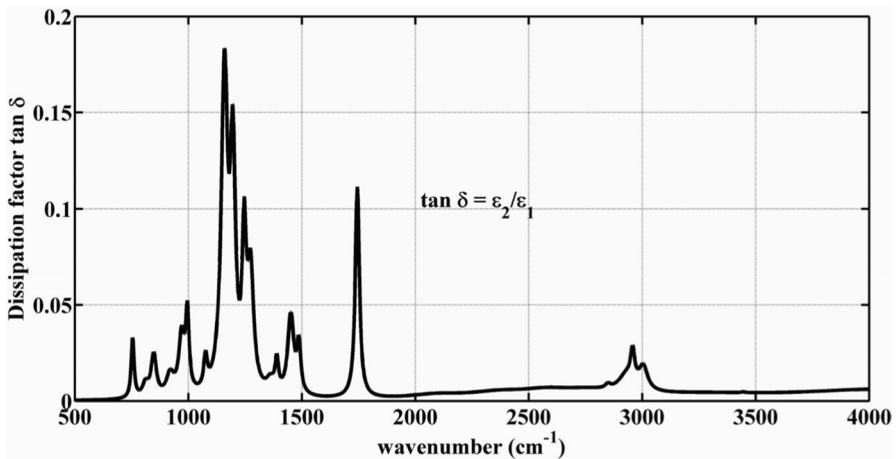


Fig. 7 Infrared spectrum of the dissipation factor $\tan \delta$ of the poly(methyl methacrylate) film cast on the metal mirror

the frequency of radiation and the extinction coefficient k . For this reason, the absorption bands from high frequencies are expected to be more intense than those in the extinction coefficient spectrum. The change in the appearance of the absorption band at 3400 cm^{-1} is better highlighted. Figure 8 shows the IR spectrum of the absorption coefficient α .

The penetration depth has an IR spectrum with an appearance different from that of the other optical properties. Figure 9 shows the IR spectrum of the penetration depth through the PMMA film cast on the metallic mirror.

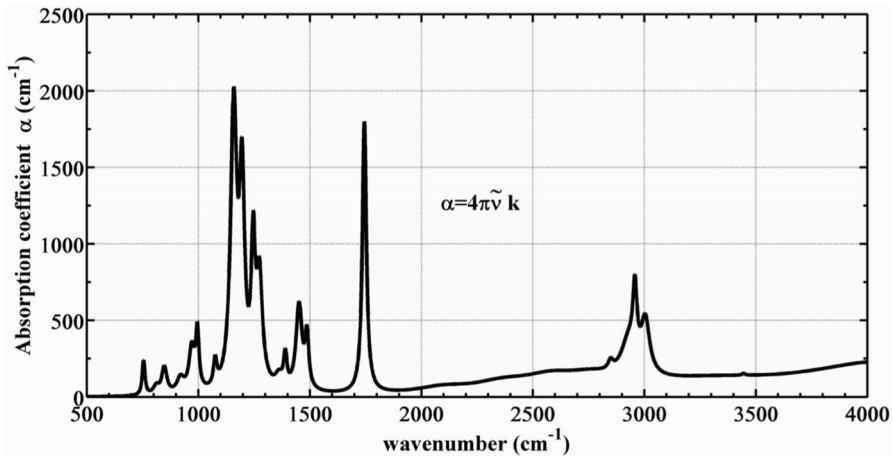


Fig. 8 Infrared spectrum of the absorption coefficient of the poly(methyl methacrylate) thin film cast on a metallic mirror obtained by classical dispersion analysis of the reflection–absorption spectrum with the RefFIT program

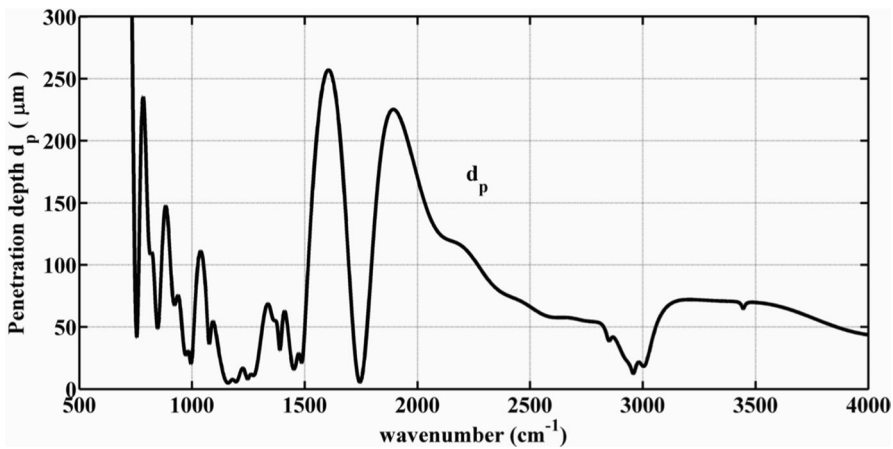


Fig. 9 Infrared spectrum of the penetration depth δ_p of radiation through a superficial poly(methyl methacrylate) film cast on a metallic mirror

In the spectral regions where the film has the highest absorption, the penetration depth of the radiation through the superficial film decreases substantially, and the absorption process is limited near the surface [22]. The penetration depth is greater than the thickness of the superficial film (5.3 μm) in almost all spectral regions. Radiation refracted at the air–film interface can reach the polymer–metal interface and is reflected on the metallic mirror (with a high reflectance coefficient $R_{23} = 0.894$) [4].

Some thermal degradation processes or polymer irradiation cause a significant decrease in the intensity of the reflection–absorption spectrum, leading to

the formation of a specular reflection spectrum rather than a reflection–absorption spectrum.

The real (σ_1) and imaginary (σ_2) infrared spectra of the optical conductivity for the PMMA layer deposited on the metal mirror are presented in Fig. 10.

The IR spectra of these two materials are similar for this reason. The optical conductivity σ_{opt} is less significant for simple polymers with dielectric properties. It is used mainly in the case of conductive polymers, called organic metal polymers, or in the case of semiconductor materials to detect the allowed interband optical transitions.

The optical properties of PMMA (ϵ_2 , M_2 , VELF, SELF, k , α , $\tan \delta$ and σ_1) which depend directly on the absorbing properties of the polymer, present similar IR spectra. The optical properties (ϵ_1 , M_1 and n) that depend on the dispersion of the radiation in the medium through which it passes also have similar IR spectra.

Conclusions

The novelty of this work is the simple way to determine the complex relative permittivity and then obtain the main optical properties of PMMA. The IRRA polymer spectra were processed using the Drude–Lorentz model and classical dispersion analysis. The real and imaginary parts of the complex relative permittivity served as a starting point for subsequently obtaining the spectra of the main optical properties of PMMA.

The obtained and presented spectra show that the IR spectra of some of the quantities presented have similar appearances. The extinction coefficient k , the absorption coefficient α , the real part of the conductivity σ_1 , the imaginary part of the complex electric modulus M_2 , the surface energy loss function SELF, and

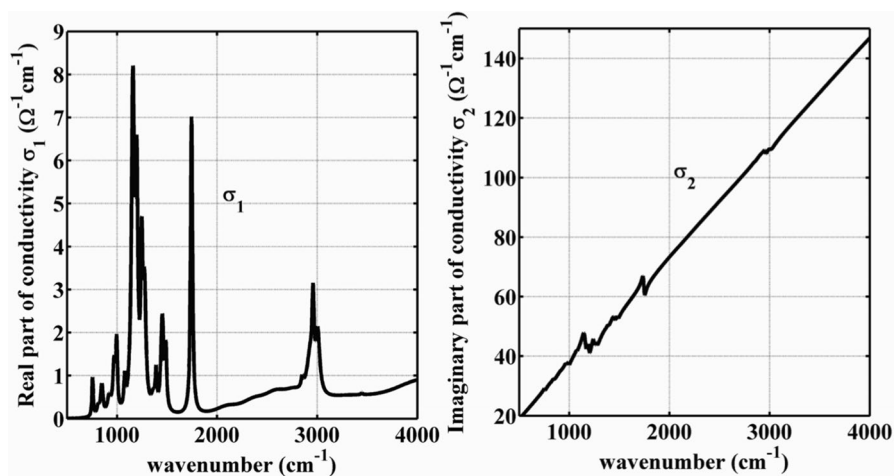


Fig. 10 Infrared spectra of the real part σ_1 and the imaginary part σ_2 of the optical conductivity for the superficial poly(methyl methacrylate) film cast on a metallic mirror

the dielectric loss tangent $\tan \delta$ all have IR spectra that resemble the imaginary part of the complex permittivity ε_2 . For this reason, Jitian and Bratu [4] only presented the change in the IR spectrum aspect of the extinction coefficient k during UV irradiation of the PMMA film. This change was considered sufficient to highlight polymer transformations. The spectra of the real part of the complex electric modulus M_1 and of the refractive index n are similar to those of the real part of the complex permittivity ε_1 . Because of this, it is sufficient to track only the IR spectrum of the refractive index n . The optical properties (ε_1 , M_1 and n) of the radiation in the medium through which it passes also have similar IR spectra. Most of the related articles present only that depend on the dispersion the IR spectra of the optical constants n and k and their changes during different structural transformations of the polymer.

It is important to know the spectral regions where the penetration depth is less than the thickness of the surface film. If the thickness of the superficial film is greater than δ_p , there is no transfection through the superficial film. In these spectral regions, specular reflection occurs, and the appearance of the spectrum can be distorted, providing false information.

In the spectral regions where the surface film shows high absorption, large VELF/SELF ratios are observed.

Author contributions All the authors whose names appear in the submission made substantial contributions to the conception or design of the work. Conceptualization done by MLS; methodology done by SJ; formal analysis and investigation done by SJ; writing—original draft preparation done by AMB; writing—review and editing done by SGŞ. All the authors commented on previous versions of the manuscript. All the authors read and approved the final manuscript.

Funding The authors received no support from any organization for the submitted work.

Declarations

Conflict of interest The authors declare that they have no known competing financial interests or personal relationships that could have appeared to influence the work reported in this paper.

References

1. Allara D, Stapleton J (2013) Methods of IR spectroscopy for surfaces and thin films. In: Bracco G, Holst B (eds) Surface science techniques. Springer, Berlin Heidelberg, pp 59–98
2. Fringeli UP (2000) ATR and reflectance IR spectroscopy. In: Lindon JC, Tranter GE, Holmes JL (eds) Encyclopedia of spectroscopy and spectrometry. Academic Press, London, pp 58–75
3. Yamamoto K, Ishida H (1994) Optical theory applied to infrared spectroscopy. *Vib Spectrosc* 8:1–36. [https://doi.org/10.1016/0924-2031\(94\)00022-9](https://doi.org/10.1016/0924-2031(94)00022-9)
4. Jitian S, Bratu I (2022) Changing the optical properties of poly(methyl methacrylate) superficial films during UV irradiation. *Spectrosc Lett* 55:199–211. <https://doi.org/10.1080/00387010.2022.2046105>
5. Jitian S, Bratu I (2012) Determination of optical constants of polymethyl methacrylate films from ir reflection-absorption spectra. *AIP Conf Proc* 1425:26–29. <https://doi.org/10.1063/1.3681958>
6. Kuzmenko AB (2005) Kramers–Kronig constrained variational analysis of optical spectra. *Rev Sci Instrum* 76:083108. <https://doi.org/10.1063/1.1979470>

7. Berdie AD, Berdie AA, Jitian S (2021) The degradation of thin poly(methyl methacrylate) films subjected to different destructive treatments. *J Polym Res-Taiwan* 28:60. <https://doi.org/10.1007/s10965-020-02390-0>
8. Alrooqi A, Al-Amshany ZM, Al-Harbi LM, Altalhi TA, Refat MS, Hassanien AM, Atta AA (2022) Impact of charge transfer complex on the dielectric relaxation processes in poly(methyl methacrylate) Polymer. *Molecules* 27:1993. <https://doi.org/10.3390/molecules27061993>
9. Vassilikou-Dova A, Kalogeras IM (2009) Dielectric Analysis. In: Mencil JD, Bruce Prime R (eds) *Thermal analysis of polymers fundamentals and application*. Wiley and sons, New Jersey, pp 497–614
10. Kuzmenko AB (2018) Guide to ReFIT: Software to fit optical spectra <http://optics.unige.ch/alexey/refit.html>. Accessed 3 Dec 2023
11. El-Nahass MM, Soliman HS, El-Denglawey A (2016) Absorption edge shift, optical conductivity, and energy loss function of nano thermal-evaporated N-type anatase TiO₂ films. *Appl Phys A-Matter* 122:775. <https://doi.org/10.1007/s00339-016-0302-6>
12. El-Denglawey A, Makhlof MM, Dongol M, El-Nahass MM (2015) The effect of long term aging on the structural and optical properties of nano metallo-tetraphenylporphine films. *J Mater Sci-Mater El* 26:5603–5609. <https://doi.org/10.1007/s10854-015-3017-0>
13. El-Denglawey A (2018) Illumination effect on the structural and optical properties of nano meso nickel(II) tetraphenyl-21H, 23H-porphyrin films induces new two hours photo bleached optical sensor. *J Lumin* 194:381–386. <https://doi.org/10.1016/j.jlumin.2017.10.070>
14. Montecchi A, Mittiga A, Malerba C, Menchini F (2023) KSEMAW: an open source software for the analysis of spectrophotometric, ellipsometric and photothermal deflection spectroscopy measurements. *Open Research Europe* 1:95. <https://doi.org/10.12688/openreseurope.13842.1>
15. Zhang HT, He R, Peng L, Yang YT, Sun J, Zhang YS et al (2023) Interpretation of reflection and colorimetry characteristics of indium-particle films by means of ellipsometric modeling. *Nanomaterials* 13:383. <https://doi.org/10.3390/nano13030383>
16. El-Denglawey A, Dongol M, El-Nahass MM (2010) Photoinduced absorption edge shift of As₂₀Se₆₀Tl₂₀ films. *J Lumin* 130:801–804. <https://doi.org/10.1016/j.jlumin.2009.11.036>
17. El-Denglawey A, Alburaih HA, Adam MS, Dongol M, El-Nahass MM, MM et al (2021) Dependence of new environmental nano organic semiconductor nickel-(II)-tetraphenyl-21H, 23H-porphyrin films on substrate type for energy storage applications. *Int J Environ Sci Te* 18:393–400. <https://doi.org/10.1007/s13762-020-02829-3>
18. Dongol M, Abou Zied MG, Gamal A, El-Denglawey A (2004) The effects of composition and heat treatment on the structural and optical properties of Ge₁₅Te_{85-x}Cu_x thin films. *Physica B* 353:169–175. <https://doi.org/10.1016/j.physb.2004.09.092>
19. Dongol M, El-Denglawey A, Abd El Sadek MS, Yahia IS (2015) Thermal annealing effect on the structural and the optical properties of Nano CdTe films. *Optik* 126:1352–1357. <https://doi.org/10.1016/j.ijleo.2015.04.0480030-4026>
20. Al-Harbi FF, El-Nahass MM, Soliman HS, El-Denglawey A (2020) Nano structure and optical properties of two hours thermal aged AsAgS films deposited on quartz substrate: new time factor. *Opt Quant Electron* 52:368. <https://doi.org/10.1007/s11082-020-02476-5>
21. Aras G, Orhan E, Selçuk AB, Ocak SB, Ertuğrul M (2015) Dielectric properties of Al/poly(methyl methacrylate)(PMMA)/p-Si structures at temperatures below 300 K. *Proc Soc Behv* 195:1740–1745. <https://doi.org/10.1016/j.sbspro.2015.06.295>
22. Frayssinous C, Fortin V, Bérubé JP, Fraser A, Vallée R (2018) Resonant polymer ablation using a compact 3.44 μm fiber laser. *J Mater Process Tech* 252:813–820. <https://doi.org/10.1016/j.jmatp rotec.2017.10.051>
23. El-Denglawey A, Alburaih HA, Mostafa MM, Adam MSS, Makhlof MM (2021) Blueshifted dielectric properties and optical conductivity of new nanoscale nickel-(II)-tetraphenyl-21H, 23H-porphyrin films as a function of UV illumination for energy storage applications. *Opt Quant Electron* 53:343. <https://doi.org/10.1007/s11082-021-02972-2>
24. Dresselhaus MS (2001) *Solid state physics. Part II Optical properties of solids. Lecture Notes Part 2*. <http://web.mit.edu/afs/athena/course/6/6.732/www/opt.pdf>. Accessed 3 Dec.2023
25. Rashidian M, Dorrarian D (2014) Low-intensity UV effects on optical constants of PMMA film. *J Theor Appl Phys* 8:121. <https://doi.org/10.1007/s40094-014-0121-0>
26. Bhavsar VB, Tripathi D (2016) Study of refractive index dispersion and optical conductivity of PPY doped PVC films. *Indian J Pure Ap Phy* 54:105–110

27. Kumar N, Sengwa RJ, Dhatarwal P, Saraswat M (2022) Effectively polymer composition controllable optical properties of PVDF/PMMA blend films for advances in flexible device technologies. *Indian J Eng Mater S* 29:169–180
28. Aly KA (2022) Comment on the relationship between electrical and optical conductivity used in several recent papers published in the journal of materials science: materials in electronics. *J Mater Sci-Mater El* 33:2889–2898. <https://doi.org/10.1007/s10854-021-07496-9>
29. Evchuk IY, Musii RI, Makitra RG, Pristanskii RE (2005) Solubility of polymethyl methacrylate in organic solvents. *Russ J Appl Chem* 78:1576–1580. <https://doi.org/10.1007/s11167-005-0564-9>
30. Hossein Esfahani Z, Ghanipour M, Dorrani D (2014) Effect of dye concentration on the optical properties of red-BS dye-doped PVA film. *J Theor Appl Phys* 8:117–121. <https://doi.org/10.1007/s40094-014-0139-3>
31. Goktas A, Tumbul A, Aba Z, Kilic A, Aslan F (2020) Enhancing crystalline/optical quality, and photoluminescence properties of the Na and Sn substituted ZnS thin films for optoelectronic and solar cell applications; a comparative study. *Opt Mater* 107:110073. <https://doi.org/10.1016/j.optmat.2020.110073>
32. Yang H, Ren Q, Zhang G, Chow YT, Chan HP, Chu PL (2005) Preparation and optical constants of the nano-crystal and polymer composite $\text{Bi}_4\text{Ti}_3\text{O}_{12}$ /PMMA thin films. *Opt Laser Technol* 37:259–264. <https://doi.org/10.1016/j.optlastec.2004.04.004>
33. Goktas A, Tumbul A, Aba Z, Durgun M (2019) Mg doping levels and annealing temperature induced structural, optical and electrical properties of highly c-axis oriented ZnO: Mg thin films and Al/ZnO:Mg/p-Si/Al heterojunction diode. *Thin Solid Films* 680:20–30. <https://doi.org/10.1016/j.tsf.2019.04.024>
34. Tumbul A, Göktaş A, Zarbali MZ, Aslan F (2018) Structural, morphological and optical properties of the vacuum-free processed CZTS thin film absorbers. *Mater Res Express* 5:066408. <https://doi.org/10.1088/2053-1591/aac80e>
35. Goktas A, Tumbul A, Aslan F (2019) A new approach to growth of chemically depositable different ZnS nanostructures. *J Sol-Gel Sci Techn* 90:487–497. <https://doi.org/10.1007/s10971-019-04990-9>
36. Şerban SG, Strugariu LM, Jitian S (2023) The influence of solvents on the appearance of the absorption bands of the polystyrene films deposited from solutions on metal mirrors. *Opt Appl* 53:5–19. <https://doi.org/10.37190/oa230101>

Publisher's Note Springer Nature remains neutral with regard to jurisdictional claims in published maps and institutional affiliations.

Springer Nature or its licensor (e.g. a society or other partner) holds exclusive rights to this article under a publishing agreement with the author(s) or other rightsholder(s); author self-archiving of the accepted manuscript version of this article is solely governed by the terms of such publishing agreement and applicable law.